Amplified random fiber laser-pumped mid-infrared optical parametric oscillator

Yaping Shang (尚亚萍)[1,2,3], Meili Shen (沈梅力)[1,2,3], Peng Wang (王 鹏)[1,2,3], Xiao Li (李 霄)[1,2,3,4,*], and Xiaojun Xu (许晓军)[1,2,3,]**

[1]*College of Optoelectric Science and Engineering, National University of Defense Technology, Changsha 410073, China*
[2]*Hunan Provincial Key Laboratory of High Energy Laser Technology, Changsha 410073, China*
[3]*Hunan Provincial Collaborative Innovation Center of High Power Fiber Laser, Changsha 410073, China*
[4]*State Key Laboratory of Crystal Materials, Shandong University, Jinan 250100, China*
**Corresponding author: crazy.li@163.com; **corresponding author: xuxj@21cn.com*
Received July 14, 2016; accepted October 14, 2016; posted online November 14, 2016

In this Letter, we report, for the first time to our knowledge, on a continuous-wave, singly resonant optical parametric oscillator using an MgO: PPLN crystal pumped by an all-fiberized master-oscillator power amplifier structured amplified random fiber laser. An idler output power of 2.46 W at 3752 nm is achieved with excellent beam quality, and the corresponding pump-to-idler conversion efficiency is 9.6% at room temperature. The idler output power exhibits a peak-to-peak power stability better than 12.7%, and the corresponding standard deviation is better than 3.6% RMS in about 20 min at the maximum output power. Meanwhile, other characteristics of the generated signal and idler laser are studied in detail and not only offered an effective guide in the research of optical parametric processes in the case of a continuous spectrum, but also broadened the range of random fiber laser applications.

OCIS codes: 190.4975, 190.4970.
doi: 10.3788/COL201614.121901.

Many applications, such as environmental monitoring, high-resolution molecular spectroscopy, and infrared countermeasures, require mid-infrared (MIR) sources operating in the 3–5 μm wavelength range[1–3]. Optical parametric oscillators[4–20] (OPOs), especially fiber laser-pumped MgO: PPLN OPOs[10–20], provide an effective approach to generate MIR lasers for their compact volume, electrical operation, and high conversion efficiency, which have attracted the interest of many researchers. In 2014, we reported the highest continuous-wave (CW) output power of 34.2 W at 3.35 μm from an MgO: PPLN OPO, which was pumped by a homemade quasi-single-frequency (SF) Yb-doped fiber laser[21]. A higher idler laser is hard to obtain. One potential reason for this is that the nonlinearity effect (such as the self-pulsation effect) has a significant influence on the performances of conventional fiber lasers under high power output scaling, such as spectral broadening, temporal instability, and intensity fluctuations[22,23]. All of these would have unfavorable influences on the following optical parametric processes, including the power instability and low pump-to-idler conversion efficiency, which prevents OPOs from further power scaling.

Recently, the concept of random fiber lasers (RFLs) has attracted a great deal of attention for its ability to generate incoherent light free from mode competition without a traditional laser resonator and ensure the stationary narrow-band continuous modeless spectrum[24–30]. The RFLs took a big step forward when, in the year 2010[24], a random distributed feedback (RDFB) fiber laser based on Raman amplification and distributed Rayleigh scattering feedback in a single-mode fiber (SMF) was reported. Since then, more and more scholars have been committed to the research in this field. In 2015, Du *et al.*[29] demonstrated a kW-class fiber amplifier seeded by an RFL with a spectral-broadening-free property caused by the temporal stability of the RFL seed, which was quite different from a traditional high-power fiber amplifier. Early this year, Dontsova *et al.*[30] reported the first experimental study of frequency doubling an RFL in an MgO: PPLN crystal, and by contrast, the highest second harmonic generation (SHG) efficiency was obtained for the RDFB Raman fiber laser with the fiber Bragg grating (FBG). On these bases, the corresponding experiments of a singly resonant optical parametric oscillator (SRO) pumped by a high-power, all-fiberized, master oscillator power amplifier (MOPA)-configuration-amplified RFL were carried out.

In this Letter, we reported on, to our knowledge, what was the first experimental demonstration of an SRO pumped by an amplified RFL. The characteristics of the generated signal and idler laser have been studied in detail. The experimental results were of great interest in terms of both the investigation of optical parametric processes in the case of a continuous spectrum and the extension of the range of RFL applications.

An experimental schematic diagram of the amplified RFL-pumped MIR OPO system is illustrated in Fig. 1. The OPO was pumped by a homemade high-power nonlinearly polarized 1070 nm amplified RFL, which was composed of a half-cavity structure, temporally stable RDFB Raman fiber laser and a high-power fiber amplifier stage, similar to the MOPA described in Ref. [29], except that the gain fiber used in the amplifier was characterized

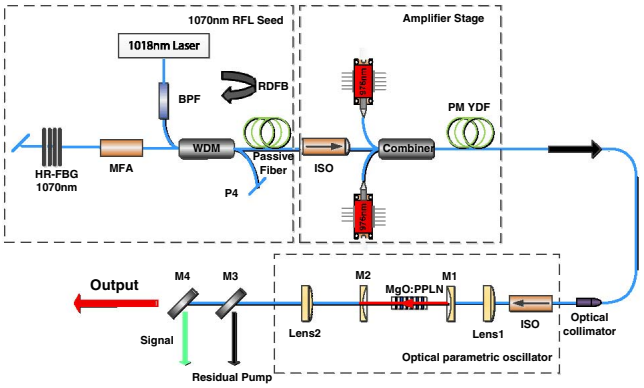

Fig. 1. Schematic diagram of experimental setup. HR-FBG, high-reflectivity FBG; MFA, mode field adapter; BPF, band-pass filter; WDM, wavelength division multiplexer; P4, extra port of WDM.

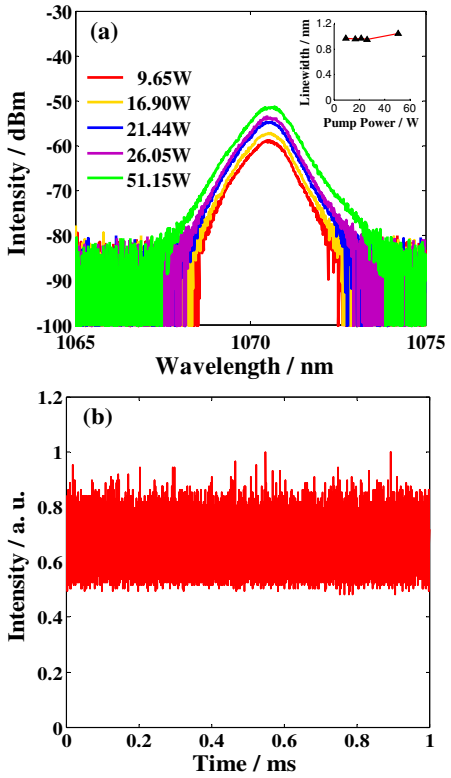

Fig. 2. Characteristics of the amplified RFL. (a) Detailed spectrum varying with different output powers. (b) Temporal stability at full power.

by polarization-maintaining (PM) physical properties according to the existing experimental conditions. Both the seed laser and amplifier system had been successfully established by using a standard SMF (10/125 μm, core diameter/inner cladding). The output fiber laser was collimated by an optical fiber collimator. Due to the nonlinearly polarized seed source and the nonlinearly polarized fiber isolator, a nonlinearly polarized beam of 4 mm in diameter in the TEM_{00} spatial mode was finally obtained.

In the experiment, a maximal nonlinearly polarized output power of 51.2 W was obtained. It should be noted that the amount of two orthogonally polarized directions' output powers were measured by using a polarized beam splitter (PBS). The measured results showed that the polarization splitting ratio of the output laser was about 1:1, which meant that the actual pump power used in the following frequency conversion processes was only about 25.6 W. There was no effort made to polarize the pump laser in the experiment, considering the optimized configuration and easy operation.

The corresponding spectrum of the amplified RFL at different output powers is charted in Fig. 2(a). The output spectrum was centered at 1070 nm with a maximum output power of 51.2 W. The full width at half-maximum (FWHM) spectrum linewidth as a function of the output power is depicted in the graph in Fig. 2(a), where it can be seen that the spectrum linewidth has almost had no broadening varying with the output power. Figure 2(b) (detected by a Thorlab InGaAs detector with a bandwidth of 180 MHz and a Tektronix oscillograph with a bandwidth of 1 GHz) shows the temporal stability of the amplified RFL at the maximal output power under a 100 μs resolution, which illustrates that no self-pulsing effect was observed in the amplified RFL.

The nonlinearly polarized output power of the amplified RFL was then passed through an optical isolator to protect the pumping source from OPO's back reflections and back conversions, and then it was focused into the OPO cavity with a beam radius of 48 μm at the center of the crystal. The OPO cavity was designed to be a simple linear, singly resonant signal with a couple of plane-concave mirrors (M1 and M2) based on a 50 mm long MgO: PPLN crystal (HC Photonics) with a 4 mm × 1 mm aperture, which was anti-reflection coated for the pump, signal, and idler lasers. The quasi-phase-matched (QPM) poling period was $\Lambda = 29.8$ μm. The input mirror M1 had a high reflectivity ($R > 99.9\%$) over 1.4–1.7 μm and was anti-reflection coated for the pump from 1.0–1.1 μm and the idler from 2.5–4.1 μm. The coupling output mirror M2 was coated with partial transparency around the signal laser in the 1.4–1.7 μm wavelength region. A convex-plane lens was used to collimate the output laser in order to ensure the measurements were accurate. In fact, the idler, signal, and residual pump laser were coupled out through the output coupler. Two dichroic mirrors were utilized after the collimating lens for separating the three kinds of lasers from each other. Firstly, M3 had a high reflectivity ($R > 99.9\%$) over the pump from 1.0–1.1 μm and was anti-reflection coated for signal from 1.4–1.7 μm and the idler from 2.5–4.1 μm; thus, the pump laser was separated from the signal and idler lasers. Additionally, M4 had high reflectivity coating for the signal and high transmission for the idler, and then the signal laser was separated from the idler laser. Three power meters were used to measure the power of the un-depleted pump laser, the signal laser, and the idler laser.

The measured idler output power of the OPO system as a function of the pump power is shown in Fig. 3(a). As can be seen, the OPO realized a maximum idler output power of 2.46 W for given 25.6 W linearly polarized pump power with a corresponding conversion efficiency of 9.6% and a threshold of 18 W under the novel pumping source. The oscillator threshold power of the OPO was relatively high. One potential reason for this is that the pump source had a broad linewidth of 0.9 nm, which resulted in a low power spectral density. Meanwhile, a signal power of 4.88 W was obtained, and the total conversion efficiency was up to 28.7%. Figure 3(b) shows the power stability of the idler laser at a high-power operation. The peak-to-peak power fluctuation was computed as being 12.7%, and the standard deviation was better than 3.6% RMS in about 20 min, as was that of the OPO pumped by a conventional fiber laser[16]. The idler power fluctuation was mainly from the environmental changes in the laboratory because the whole system, including the fiber MOPA and the OPO, was simply air cooled. The graph in Fig. 3(b) shows the temporal stability of idler laser at a high-power operation in the μs-class domain. It is clearly seen that the idler laser had good temporal stability, as did the pumping source.

Figure 4(a) shows the optical signal spectrum at the maximal power scaling of the OPO using the optical spectrum analyzer. The signal spectrum was centered at 1498 nm with an FWHM linewidth of 0.14 nm, which presented a wavelength shift for repeat measurements. One possible reason was that the extremely weak temperature rise of the nonlinear crystal resulted in a new phase-matching condition. Meanwhile, the optical idler spectrum at the maximum output power of the OPO using an MIR wavelength meter (Bristol, 621 A) is shown in

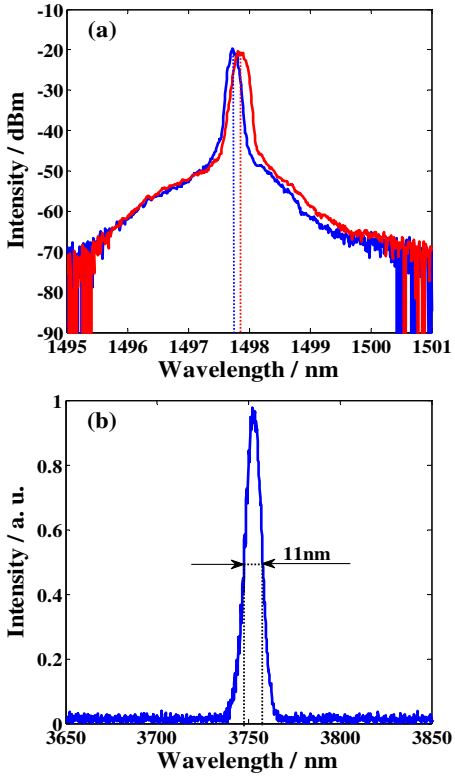

Fig. 4. Spectra details of (a) signal laser and (b) idler laser.

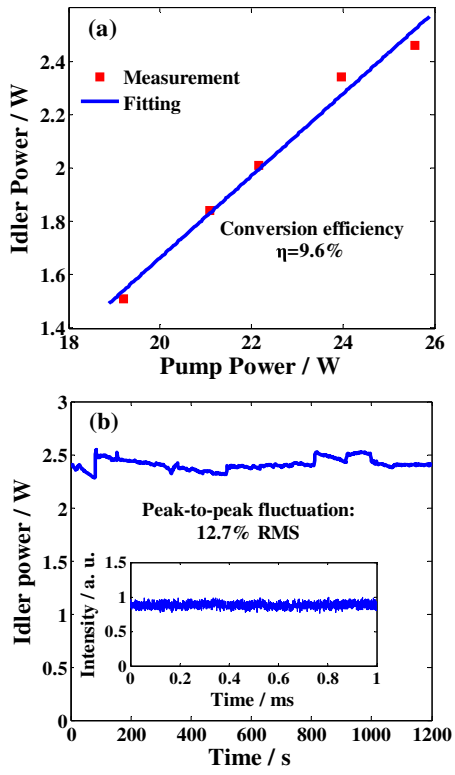

Fig. 3. Characteristics of the idler laser. (a) Output power as a function of the pump power. (b) Temporal stability.

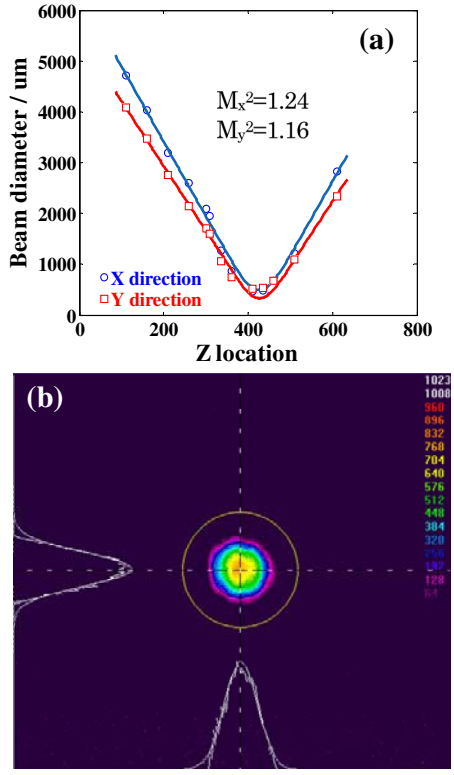

Fig. 5. (a) Beam quality measurement. (b) Near-field intensity distribution of the idler laser.

Fig. 4(b). The idler spectrum was centered at 3752 nm with an FWHM linewidth of 11 nm.

The beam quality of the idler laser at the maximum output power pumped by the amplified RFL was measured with knife-edge method by Ophir-Spiricon beam propagation analyzer software with a pyrocam-III, as depicted in Fig. 5(a). The beam quality M^2 factors were ~1.24 and ~1.16 in the horizontal and vertical directions, respectively. Figure 5(b) shows the corresponding beam near-field intensity distribution of the mid-infrared laser at the maximum output power.

In conclusion, we report on, to our knowledge, what is the first experimental demonstration of an SRO pumped by an amplified RFL. An idler power of 2.46 W at 3752 nm is achieved with good beam qualities of $M_x^2 = 1.24$ and $M_y^2 = 1.16$ under the highest pump power, and the corresponding pump-to-idler conversion efficiency is 9.6% at room temperature. The idler output power exhibits a peak-to-peak power stability better than 12.7%, and the standard deviation is better than 3.6% RMS in about 20 min at the maximum output power. Meanwhile, other characteristics of the generated signal and idler laser are studied in detail. These are of great interest in terms of both the investigation of optical parametric processes in the case of a continuous spectrum and the extension of the range of RFL applications.

The authors would like to thank Master Xueyuan Du and Dr. Hanwei Zhang for their kind assistance with the RFL seed source.

References

1. U. Willer, M. Saraji, A. Khorsandi, P. Geiser, and W. Schade, Opt. Lasers Eng. **44**, 699 (2006).
2. M. Vainio, M. Siltanen, J. Peltola, and L. Halonen, Appl. Opt. **50**, A1 (2011).
3. R. Tuttle, Aerosp. Daily Defense Rep. **210**, 6 (2004).
4. X. P. Hu, P. Xu, and S. N. Zhu, Photon. Res. **1**, 171 (2013).
5. L. Xia, H. Su, and S. Ruan, Chin. Opt. Lett. **7**, 1038 (2009).
6. X. Wei, Y. Peng, W. Wang, and X. Chen, Chin. Opt. Lett. **8**, 1061 (2010).
7. W. Tian, J. Zhu, Z. Wang, and Z. Wei, Chin. Opt. Lett. **13**, 011901 (2015).
8. S. Li, P. Ju, Y. Liu, X. Jiang, R. Ni, G. Zhao, X. Lv, and S. Zhu, Chin. Opt. Lett. **14**, 041402 (2016).
9. Q. Mo, S. Li, Y. Liu, X. Jiang, G. Zhao, Z. Xie, X. Lv, and S. Zhu, Chin. Opt. Lett. **14**, 091902 (2016).
10. L. Xu, H.-Y. Chan, S.-U. Alam, D. J. Richardson, and D. P. Shepherd, Opt. Lett. **40**, 3288 (2015).
11. P. Jiang, T. Chen, B. Wu, D. Yang, C. Hu, P. Wu, and Y. Shen, Opt. Express **23**, 2633 (2015).
12. D. W. Chen and T. S. Rose, in *Conference on Lasers and Electro-Optics* (Optical Society of America, 2005), paper CThQ2.
13. L. Wang, Q. Liu, E. Ji, H. Chen, and M. Gong, Appl. Opt. **53**, 6729 (2014).
14. K. Devi, S. C. Kumar, and M. Ebrahim-Zadeh, Opt. Lett. **37**, 5049 (2012).
15. A. Henderson and R. Stafford, Opt. Express **14**, 767 (2006).
16. S. Chaitanya Kumar and M. Ebrahim-Zadeh, Opt. Lett. **36**, 2165 (2011).
17. P. Jiang, T. Chen, D. Yang, B. Wu, S. Cai, and Y. Shen, Laser Phys. Lett. **10**, 115405 (2013).
18. J. B. Barria, S. Roux, J. B. Dherbecourt, M. Raybaut, J. M. Melkonian, and A. Godard, Opt. Lett. **38**, 2165 (2013).
19. T. Chen, K. Wei, P. Jiang, B. Wu, and Y. Shen, Appl. Opt. **51**, 6881 (2012).
20. T. Chen, P. Jiang, and D. Yang, Appl. Opt. **52**, 6316 (2013).
21. X. Li, X. Xu, Y. Shang, H. Wang, and L. Liu, Proc. SPIE **9251**, 92510A (2014).
22. S. K. Turitsyn, A. E. Bednyakova, M. P. Fedoruk, A. I. Latkin, A. A. Fotiadi, A. S. Kurkov, and E. Sholokhov, Opt. Express **19**, 8394 (2011).
23. B. N. Upadhyaya, U. Chakravarty, A. Kuruvilla, S. M. Oak, M. R. Shenoy, and K. Thyagarajan, Opt. Commun. **283**, 2206 (2010).
24. S. K. Turitsyn, S. A. Babin, A. E. El-Taher, P. Harper, D. V. Churkin, S. I. Kablukov, J. D. Ania-Castañón, V. Karalekas, and E. V. Podivilov, Nat. Photon. **4**, 231 (2010).
25. B. Redding, M. A. Choma, and H. Cao, Nat. Photon. **6**, 355 (2012).
26. J. H. Lee, Y. M. Chang, Y. G. Han, H. Chung, S. H. Kim, and S. B. Lee, Opt. Express **12**, 3515 (2004).
27. D. S. Wiersma, Nat. Phys. **4**, 359 (2008).
28. A. A. Fotiadi, Nat. Photon. **4**, 204 (2010).
29. X. Du, H. Zhang, P. Ma, H. Xiao, X. Wang, P. Zhou, and Z. Liu, Opt. Lett. **40**, 1 (2015).
30. E. I. Dontsova, S. I. Kablukov, I. D. Vatnik, and S. A. Babin, Opt. Lett. **41**, 1439 (2016).